Journal of Alloys and Compounds 489 (2010) L4–L8

Contents lists available at ScienceDirect

Journal of Alloys and Compounds

journal homepage: www.elsevier.com/locate/jallcom

Letter

Properties and rapid consolidation of ultra-hard tungsten carbide

In-Jin Shon[a,b,*], Byung-Ryang Kim[a], Jung-Mann Doh[c], Jin-Kook Yoon[c], Kee-Do Woo[a,b]

[a] Division of Advanced Materials Engineering and the Research Center of Advanced Materials Development, Engineering College, Chonbuk National University, JeonJu 561-756, South Korea
[b] Department of Hydrogen and Fuel Cells Engineering, Specialized Graduate School, Chonbuk National University, JeonJu 561-756, South Korea
[c] Advanced Functional Materials Research Center, Korea Institute of Science and Technology, PO Box 131, Cheongryang, Seoul 130-650, Republic of Korea

ARTICLE INFO

Article history:
Received 2 July 2009
Received in revised form 8 September 2009
Accepted 9 September 2009
Available online 16 September 2009

Keywords:
Nanostructured materials
Powder metallurgy
Mechanical properties
Sintering

ABSTRACT

Extremely dense WC with a relative density of up to 99% was obtained within 3 min under a pressure of 80 MPa using the high frequency induction heating sintering method (HFIHS) method. The average grain size of the WC was about 87 nm. The advantage of this process is not only rapid densification to obtain a near theoretical density but also the prohibition of grain growth in nanostructured materials. The hardness and fracture toughness of the dense WC produced by the HFIHS were investigated.

1. Introduction

The attractive properties of tungsten carbides include their high melting point (a peritectic melting temperature of 2785 °C), high hardness (2854 kg/mm^2), high thermal and electrical conductivities, and relatively high chemical stability [1,2]. Tungsten carbides are primarily used as cutting tools and abrasive materials in the form of composites with a binder metal such as Co or Ni. However, the binder phases have inferior chemical characteristics compared to the carbide phase. Most notably, corrosion and oxidation preferentially occur in the binder phase [3]. Hence, WC–TiC–TaC binderless cemented carbides have been developed for use in mechanical seals and sliding parts due to their enhanced corrosion resistance [4]. TiC has been used as a carbide binder because it forms a WC–TiC solid solution [5]. However, in the case of WC–TiC–TaC binderless cemented carbide, carbon segregation occurs at the grain boundaries between the WC and TiC grains, resulting in a decrease in the wear resistance and toughness of the materials [6,7]. Therefore, developing pure WC has been intensively investigated in recent years. Recently, Cha and Hong [8] reported that the gross carbon content of WC powder as well as the sintering cycle plays a critical role in controlling abnormal WC grain growth of binderless WC during spark plasma sintering (SPS). SPS has been reported to allow full densification of binderless WC within 8 min at 1300–1600 °C and 60 MPa, resulting in an ultra-fine WC grain size of 0.2 μm [9]. On the other hand, Shon and co-workers [10] investigated pure WC using high frequency induction combustion synthesis from milled elemental W and C powders. A maximum Vickers hardness of 26.54 GPa was obtained for a dense 0.43 μm sized WC grade. Using pulsed current activated sintering, nearly fully dense binderless WC with a grain size of 0.43 μm was obtained within 2 min, resulting in a Vickers hardness of 24.3 GPa [11]. Munir and co-workers [12] investigated binderless WC with minor W_2C from nanopowder WC using SPS. A maximum Vickers hardness of 26.8 GPa was obtained for a dense 305 nm sized WC grade.

Nanostructured materials have been widely investigated because they have wide functional diversity and exhibit enhanced or different properties compared to their bulk counterparts [13]. Particularly, in the case of nanostructured ceramics, the presence of a large fraction of grain boundaries can lead to unusual or better mechanical, electrical, optical, sensing, magnetic, and biomedical properties [14–19]. Recently, nanocrystalline powders have been developed by co-precipitation, a thermochemical and thermomechanical method referred to as the spray conversion process (SCP), and high energy mechanical milling (HEMM) [20,21]. However, in the conventional sintering process, the grain size in the sintered materials becomes larger than that in the pre-sintered powders due to the fast grain growth that occurs. Even though the initial particle size is less than 100 nm, the grain size increases rapidly up to 500 nm during the conventional sintering process [22]. Therefore, controlling grain growth during sintering is one of the keys to

* Corresponding author at: Division of Advanced Materials Engineering and the Research Center of Advanced Materials Development, Engineering College, Chonbuk National University, JeonJu 561-756, South Korea. Tel.: +82 63 2381; fax: +82 63 270 2386.
E-mail address: ijshon@chonbuk.ac.kr (I.-J. Shon).

0925-8388/$ – see front matter © 2009 Elsevier B.V. All rights reserved.
doi:10.1016/j.jallcom.2009.09.040

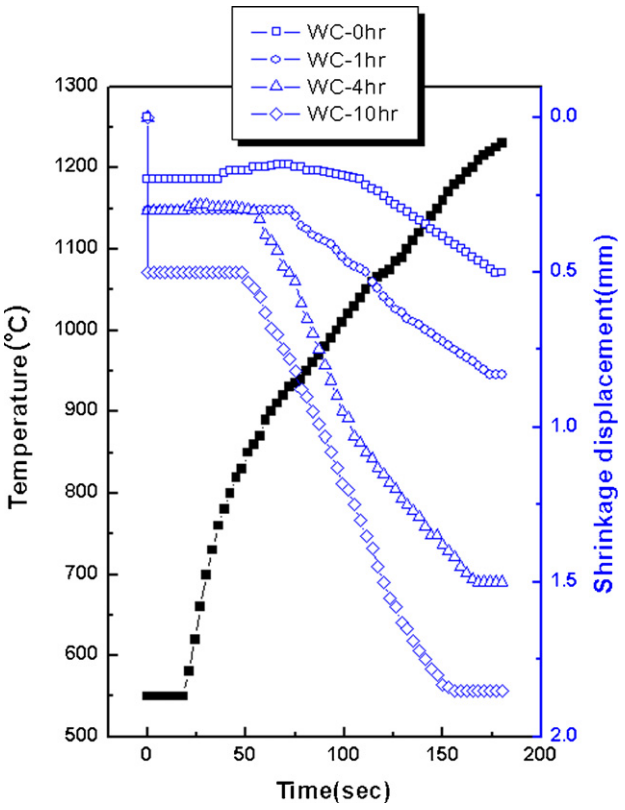

Fig. 1. Variations of temperature and shrinkage as a function of heating time during the sintering of the binderless WC powder with millings times of 0 h, 1 h, 4 h, and 10 h.

the commercial success of nanostructured materials. In this regard, the high frequency induction heating sintering method (HFIHS), which can make dense materials within 2 min, has been shown to be effective to control grain growth [23–26].

In this study, we investigated the sintering of WC obtained from mechanically activated powder by the HFIHS method without the use of a binder and analyzed the mechanical properties of binderless nanostructured WC.

2. Experimental procedures

The binderless tungsten carbide powder with a grain size of 1.3 μm used in this research was supplied by TaeguTec Ltd. (Taegu, Korea). The powder was first milled in a high energy ball mill (Pulverisette-5 planetary mill) at 250 rpm for various lengths of time (0, 1, 4, 10 h). Tungsten carbide balls (8.5 mm in diameter) were used in a sealed cylindrical stainless steel vial under an argon atmosphere. The weight ratio of the balls to the powder was 30:1. Milling resulted in a significant reduction of the grain size. The grain sizes of the WC was calculated from the full width at half-maximum (FWHM) of the diffraction peak using the formula developed by Suryanarayana and Grant Norton [27]. The average grain sizes of the WC milled for 1, 4, and 10 h determined using their formula were about 146, 54, and 40 nm, respectively.

After milling, the powders were placed in a graphite die (outside diameter of 45 mm, inside diameter of 20 mm, and height of 40 mm) and were then introduced into the HFIHS apparatus [2]. The HFIHS apparatus includes a 15 kW power supply which provides an induced current through the sample and applies a 50 kN uniaxial load. The system was first evacuated and a uniaxial pressure of 80 MPa was applied. The induced current was then activated and maintained until the densification rate was negligible, as indicated by the real-time output of the shrinkage of the sample. The shrinkage was determined by a linear gauge measuring vertical displacement. The temperatures were measured by a pyrometer focused on the surface of the graphite die. At the end of the process, the induced current was turned off and the sample was cooled to room temperature. The process was carried out under a vacuum of 4×10^{-2} Torr.

The relative density of the sintered sample was measured by the Archimedes method. Microstructural information was obtained from product samples, which were polished and etched using Murakami's reagent (10 g potassium ferricyanide, 10 g NaOH, and 100 mL water) for 1–2 min at room temperature. Compositional and microstructural analyses of the products were made by X-ray diffraction

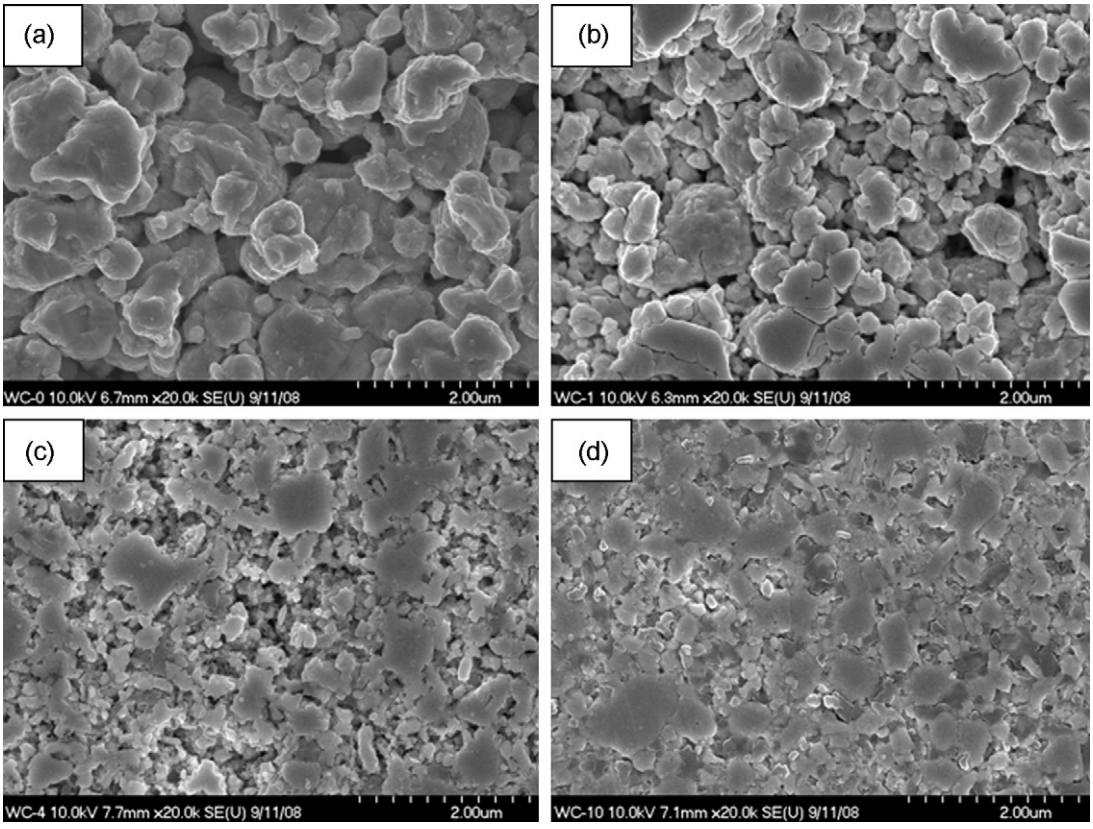

Fig. 2. FE-SEM micrographs of the pure WC sintered from the powders milled for (a) 0 h, (b) 1 h, (c) 4 h, and (d) 10 h.

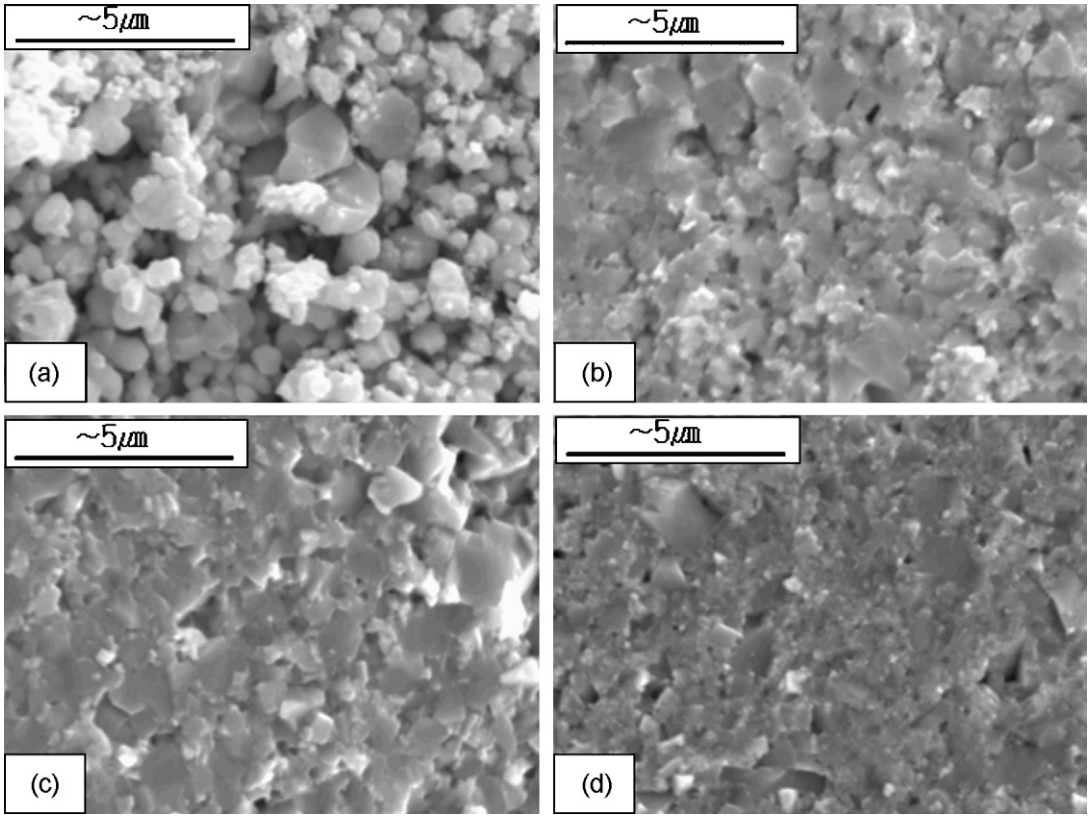

Fig. 3. SEM images of the fracture surface of WC after sintering of the powders milled for (a) 0 h, (b) 1 h, (c) 4 h, and (d) 10 h.

(XRD), scanning electron microscopy (SEM), and energy dispersive spectroscopy (EDS).

3. Results and discussion

Variation of the shrinkage displacement and temperature as a function of heating time for 80% of the total output power capacity (15 kW) during the sintering of the high energy ball milled WC under a pressure of 80 MPa is shown in Fig. 1. In all cases, the application of the induced current resulted in shrinkage due to consolidation. The shrinkage initiation temperature varied from 820 to 1020 °C depending on the milling time. The temperature at which shrinkage began decreased with increasing milling time. Also, the high energy ball milling affected the rate of densification and the final density, as will be discussed below. Figs. 2 and 3 show the effect of the ball milling time on the microstructure and fracture surfaces of the WC sintered under a pressure of 80 MPa and an induced current of 80% of the total output power capacity. In the figures, the volume of the pores decreased with milling time and few pores were detected in the WC sintered from the powder milled for 10 h. The average grain sizes of the WC calculated from the XRD data were about 732, 147, 106, and 87 nm for the samples with milling times of 0, 1, 4, and 10 h and their corresponding densities were approximately 72%, 91%, 98%, and 99%, respectively. Thus, the average grain size of the sintered WC was roughly the same as that of the initial powder, indicating the absence of grain growth during sintering. This retention of the grain size is attributed to the high heating rate and the relatively short exposure of the powders to the high temperature. As the initial particle size of the WC powder increased, the porosity also increased. A FE-SEM image of WC sintered from the 10 h milled powder is shown in Fig. 4. It is confirmed that the sintered sample consists of a nanophase of WC.

The use of spark plasma sintering (SPS) to successfully consolidate WC powders (without a binder) has been demonstrated in several investigations. In a recent work, unmilled 40–70 nm WC powders were consolidated at 1500 °C to a relative density of up to 95.5% under a pressure of 126 MPa and a current of 3000 A [12]. Comparing the results of the above study with ours, the sintering temperature of the high energy mechanical milled WC is lower then that of the unmilled powder due to the increase in the reactivity of the powder, the internal and surface energy, and the surface area, which all contribute to its mechanical activation [28–31].

Fig. 5 shows the XRD patterns of the WC after sintering for all four powders used in this work. No peaks corresponding to sub-

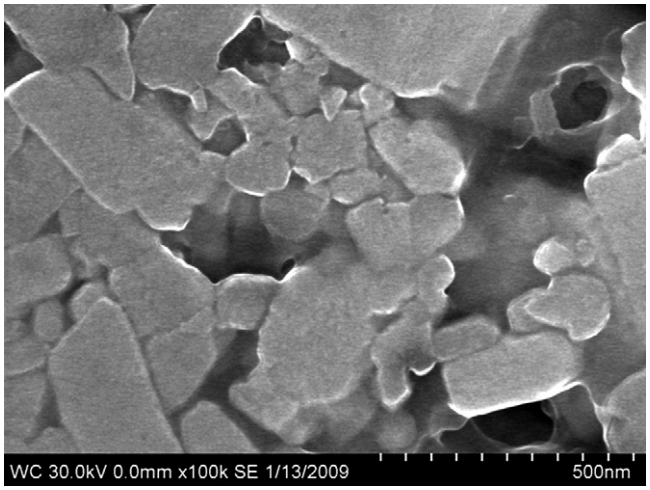

Fig. 4. FE-SEM image of the WC sintered from the powders milled for 10 h.

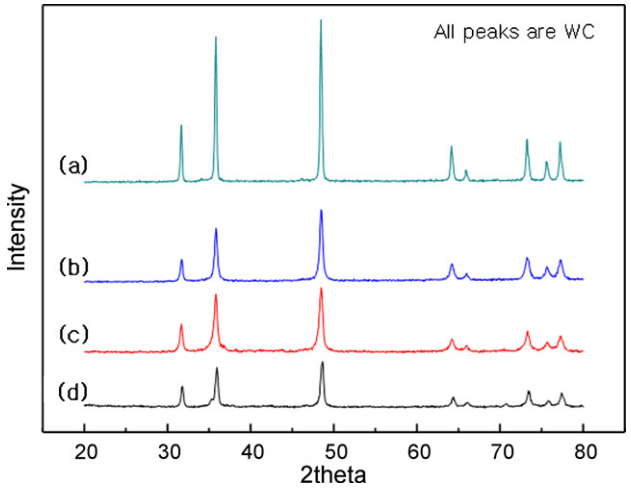

Fig. 5. XRD patterns of the binderless WC sintered from the powders milled for (a) 0 h, (b) 1 h, (c) 4 h, and (d) 10 h.

carbide W_2C or any impurity phases are present. These results, however, are in contrast with other reported observations. Cha and Hong [8] reported that the density of WC sintered at 1700 °C by the SPS method decreased with decreasing initial powder particle size. This unexpected behavior was attributed to the loss of carbon during sintering with the loss being greater for smaller particles (larger surface to volume ratios). The decarburization of WC during sintering (attributed to the presence of surface oxide in the initial powders) results in the formation of W_2C and causes a decrease in the final density. To resolve this problem, Cha and Hong [8] added excess carbon. However, they showed that the excess carbon enhanced the grain growth. When 0.5 wt.% excess carbon was added to the 0.57 μm powder, the WC grains experienced significant growth by at least a factor of two, based on the micrographs from Cha and Hong's work. Thus, while the densification of WC was accomplished without binder by Cha and Hong, the initial submicrometer grain size was not maintained.

In this work, however, no evidence for the formation of W_2C in the sintered samples was observed in the XRD patterns shown in Fig. 5. Thus, the addition of carbon was not necessary to obtain nearly fully dense products. More importantly, the products retained the grain size of the initial powder, which had an average particle size of about 87 nm.

Vickers hardness measurements were performed on polished sections of the WC samples using a 10 kgf load and a 15 s dwell time. Indentations with sufficiently large loads produced radial cracks emanating from the corners of the indent. The length of these cracks permits the fracture toughness of the material to be estimated using Anstis' expression [32]. The Vickers hardnesses of the WC with ball milling for 4 and 10 h were 2635 and 3020 kg mm^{-2}, and their fracture toughnesses were 8.3 and 7.1 MPa m$^{1/2}$, respectively. These values represent the average of 10 measurements. Table 1 provides a comparison of the hardness and fracture toughness values obtained in this work with those reported by other researchers for binderless WC [12,33,34,35]. In a previous work by Cha and Hong [8] in which binderless WC was sintered, no mechanical characterization of the products was reported. From Table 1, it can be seen that the hardness and fracture toughness values of the samples produced in this study are the highest due to refinement of the grain size.

Table 1
Comparison of the mechanical properties of the WC sintered in this study with previously reported values.

Ref.	Relative density (%)	Grain size (nm)	H_V (kg mm^{-2})	K_{1C} (MPa m$^{1/2}$)
[33]	98.5	380	2854	7.1
[12]	95.5	254	2414	–
	100	305	2730	–
[34]	98.5	430	2708	4.8
[35]	97.5	360	2479	6.6
This work	99	87	3020	7.1

The role of the current inductive in sintering or synthesis has been the focus of several studies aimed at providing an explanation of the observed enhancement of the sintering process and improved characteristics of the products. The role of the current has been interpreted differently with the effect being explained in terms of the fast heating rate due to Joule heating, the presence of a plasma in the pores separating the powder particles [36], and the intrinsic contribution of the current to mass transport [37–39].

4. Summary

In summary, nanostructured WC was sintered from mechanically activated WC powder by high frequency induction heated sintering within 3 min. The Vickers hardness and fracture toughness of the WC were 3020 kg mm^{-2} and 7.1 MPa m$^{1/2}$, respectively. These values are higher than those reported by other researchers for binderless WC due to grain refinement.

Acknowledgements

This work was supported by a Korea Science and Engineering Foundation (KOSEF) grant funded by the Korean government (MOST) (No. R01-2007-000-20002-0).

References

[1] H.C. Kim, I.J. Shon, I.K. Jeong, I.Y. Ko, J.K. Yoon, J.M. Doh, Met. Mater. Int. 13 (2007) 39–45.
[2] L.E. Toth, Transition Metal Carbides and Nitrides, Academic Press, New York, 1971.
[3] H. Suzuki, Cemented Carbide and Sintered Hard Materials, Maruzen, Tokyo, 1986, pp. 10–25.
[4] H. Suzuki, Cemented Carbide and Sintered Hard Materials, Maruzen, Tokyo, 1986, pp. 35–51.
[5] S. Imasato, K. Tokumoto, T. Kitada, S. Sakaguchi, Int. J. Refract. Met. Hard Mater. 13 (1995) 305–312.
[6] H. Engqvist, G.A. Botton, N. Axen, S. Hogmark, Int. J. Refract. Met. Hard Mater. 16 (1998) 309–313.
[7] H. Engqvist, G.A. Botton, N. Axen, S. Hogmark, J. Am. Ceram. Soc. 83 (2000) 2491–2496.
[8] S.I. Cha, S.H. Hong, Mater. Sci. Eng. A 356 (2003) 381–389.
[9] B. Huang, L.D. Chen, S.Q. Bai, Scripta Mater. 54 (2006) 441–445.
[10] H.C. Kim, I.J. Shon, J.K. Yoon, S.K. Lee, Z.A. Munir, Int. J. Refract. Met. Hard Mater. 24 (2006) 202–209.
[11] H.C. Kim, I.J. Shon, J.K. Yoon, S.K. Lee, J.M. Doh, Int. J. Refract. Met. Hard Mater. 25 (2007) 46–52.
[12] J. Zhao, T. Holland, C. Unuvar, Z.A. Munir, Int. J. Refract. Met. Hard Mater. 1 (2009) 130–139.
[13] H. Gleiter, Nanostruct. Mater. 6 (1995) 3–14.
[14] J. Karch, R. Birringer, H. Gleiter, Nature 330 (1987) 556–558.
[15] A.M. George, J. Iniguez, L. Bellaiche, Nature 413 (2001) 54–57.
[16] D. Hreniak, W. Strek, J. Alloys Compd. 341 (2002) 183–186.
[17] C. Xu, J. Tamaki, N. Miura, N. Yamazo, Sens. Actuators B 3 (1991) 147–155.
[18] D.G. Lamas, A. Caneiro, D. Niebieskikwiat, R.D. Sanchez, D. Garcia, B. Alascio, J. Magn. Mater. 241 (2002) 207–213.
[19] E.S. Ahn, N.J. Gleason, A. Nakahira, J.Y. Ying, Nano Lett. 1 (2001) 149–153.
[20] Z. Fang, J.W. Eason, Int. J. Refract. Met. Hard Mater. 13 (1995) 297–303.
[21] A.I.Y. Tok, L.H. Luo, F.Y.C. Boey, Mater. Sci. Eng. A 383 (2004) 229–234.
[22] M. Sommer, W.D. Schubert, E. Zobetz, P. Warbichler, Int. J. Refract. Met. Hard Mater. 20 (2002) 41–50.
[23] H.C. Kim, I.J. Shon, J.K. Yoon, J.M. Doh, Met. Mater. Int. 12 (2006) 141–147.
[24] H.C. Kim, I.J. Shon, I.K. Jeong, I.Y. Ko, Met. Mater. Int. 12 (2006) 393–398.
[25] D.Y. Oh, H.C. Kim, J.K. Yoon, I.J. Shon, J. Alloys Compd. 386 (2005) 270–275.
[26] H.C. Kim, D.Y. Oh, I.J. Shon, Int. J. Refract. Met. Hard Mater. 22 (2004) 41–46.
[27] C. Suryanarayana, M. Grant Norton, X-ray Diffraction A Practical Approach, Plenum Press, New York, 1998.

[28] C. Suryanarayana, Prog. Mater. Sci. 46 (2001) 1–25.
[29] F. charlot, E. Gaffet, B. Zeghmati, F. Bernard, J.C. Liepce, Mater. Sci. Eng. A 262 (1999) 279–285.
[30] V. Gauthier, C. Josse, F. Bernard, E. Gaffet, J.P. Larpin, Mater. Sci. Eng. A 265 (1999) 17–25.
[31] M.K. Beyer, H. Clausen-Schaumann, Chem. Rev. 105 (2005) 2921–2932.
[32] G.R. Anstis, P. Chantikul, B.R. Lawn, D.B. Marshall, J. Am. Ceram. Soc. 64 (1981) 533–538.
[33] H.C. Kim, J.K. Yoon, J.M. Doh, I.Y. Ko, I.J. Shon, Mater. Sci. Eng. A 435–436 (2006) 717–724.
[34] H.C. Kim, I.J. Shon, J.K. Yoon, S.K. Lee, Z.A. Munir, Int. J. Refract. Met. Hard Mater. 24 (2006) 202–207.
[35] H.C. Kim, I.J. Shon, J.E. Garay, Z.A. Munir, Int. J. Refract. Met. Hard Mater. 22 (2004) 257–263.
[36] Z. Shen, M. Johnsson, Z. Zhao, M. Nygren, J. Am. Ceram. Soc. 85 (2002) 1921–1927.
[37] J.E. Garay, U. Anselmi-Tamburini, Z.A. Munir, S.C. Glade, P. Asoka-Kumar, Appl. Phys. Lett. 85 (2004) 573–578.
[38] J.R. Friedman, J.E. Garay, U. Anselmi-Tamburini, Z.A. Munir, Intermetallics 12 (2004) 589–597.
[39] J.E. Garay, J.E. Garay, U. Anselmi-Tamburini, Z.A. Munir, Acta Mater. 51 (2003) 4487–4495.